Search for the Molecular Mechanism of Mercury Toxicity. Study of the Mercury(II)−Surfactant Complex Formation in Langmuir Monolayers

Marcin Broniatowski* and Patrycja Dynarowicz-Łatka

Faculty of Chemistry, Jagiellonian University, Ingardena 3, 30-060 Kraków, Poland

Received: November 25, 2008; Revised Manuscript Received: January 20, 2009

Surface pressure and electric surface potential measurements complemented with Brewster angle microscope observations have been used to study the interactions of Hg^{2+} ions with selected surfactants spread in Langmuir monolayers. The chosen surfactants had the same hydrocarbon chain length (18 carbon atoms) and different polar groups, such as −COOH, −NH₂, −OH, and −SH, which can be found in natural cells. Our results indicate that Hg^{2+} interacts strongly not only with the −SH group, which is believed to be the main target for mercury ions, but also with −COOH and −NH₂ groups. Another important finding is that hydracid or oxoacid mercury salts interact with surfactants differently. The observed differences were explained as being due to different coordination of mercury in the respective complexes. Similar experiments as for mercury salts have also been performed for other heavy metal ions (Cd^{2+}, Pb^{2+}, and Ag^+). It turned out that the interactions with the investigated surfactants monolayers were considerably different, which was explained by different coordination properties of the above cations. The profound changes exerted by Hg^{2+} ions on Langmuir monolayers of the selected herein surfactants (multilayer formation, induction of aggregation) may be related to natural membranes and can contribute to the elucidation of the molecular mechanism of mercury toxicity.

Introduction

Mercury, the only metal that is liquid at room temperature, is known to mankind from ancient times and the toxic properties of mercury compounds have also been known for ages.[1−4] The acute and chronic effects of mercury poisoning have been reported many centuries ago and their detailed description can be found in any book of toxicology.[5] However, even if the symptoms of mercury poisoning and the general procedures of the medical and pharmacological treatment of such cases are well-known, the molecular mechanism of mercury toxicity still remains enigmatic. The most common explanation holds that mercury binds in an unspecific way to the sulfhydryl groups of different enzymes in a rather random way, disturbing and breaking different metabolic tracts.[6] Such a statement, however, is a large oversimplification of the problem. Different hypotheses of the mechanism of mercury toxicity can be found in the literature, depending on the poisoned organ. Regarding the neurotoxicity, there was a heated debate if the methylmercury could exert the toxic effect in brain itself or if it demethylated to Hg^{2+} salts in the first step.[7] Both CH_3Hg^+ and Hg^{2+} bind to glutathione and metalothioneins, reducing the concentration of these antioxidants and causing the oxidative stress both in neurons and in the glial cells.[8,9] Moreover, CH_3Hg^+ and Hg^{2+} interfere with the calcium channels, disrupting their function, which can lead to apoptosis.[10] The interaction with the calcium channels is considered as being the most important reason for the nephro- and hepatotoxicity;[11,12] however, in these organs also the oxidative stress caused by the depletion of the glutathione and other thiols level has to be taken into account.[13] The investigations of the influence of Hg^{2+} salts on different cell lines of the canine kidney have shown that the presence of mercury causes the autoimmune reaction.[14] Also, Hg^{2+} and CH_3Hg^+ reveal hemolytic activity[15,16] and exert detrimental effects on the salivary glands.[17] The detailed analysis of the behavior of erythrocytes and isolated cell lines of the salivary gland in the presence of these mercury forms indicated that they do not interfere with the calcium channels only, but also disturb the function of water channels binding to the protein (aquaporine).[18] Water channels are abundant in erythrocytes and in cells of salivary glands; therefore, this effect can be crucial in explaining the Hg toxicity toward these cells. The acute effect of the inhalation of mercury vapors can be severe lung inflammation, and it was proved in the in vitro experiments that Hg^{2+} and CH_3Hg^+ have adverse effect on the synthesis of the lung surfactant in the alveoli.[19]

In the attempt to generalize different mechanisms of mercury toxicity, an important question arises: how do different forms of mercury cross the cell membrane; i.e., what is the interaction of Hg^{2+} and CH_3Hg^+ with the natural membrane components, such as phospholipids and proteins.[20] One of the hypothesis, so-called *molecular mimicry*,[21] holds that the structure of the complex formed by Hg^{2+} and two molecules of cysteine is very similar to its oxidized form, cystidine, and CH_3Hg^+ bound to one molecule of cysteine resembles the molecule of the amino acid, methionine; therefore, in both cases mercury in the form of complexes can cross the bilayer via the appropriate protein channels, enabling in this way the active transport of amino acids inside the cell. Mercury can also interfere with the double membrane of mitochondria and plastids, leading to the dysfunction of these organelles.[22] The interaction of mercury salts with phospholipids' vesicles as a model of cell membrane has also been performed;[23,24] however, the problem of the Hg−cell membrane components interactions remains still open and requires further studies.

Investigations regarding different properties and functions of cell membranes are often performed applying the Langmuir monolayers technique. Langmuir monolayers are formed by different kinds of water-insoluble surfactants, which are spread from a solution in a volatile organic solvent onto the water/air

* Corresponding author. Tel: +48126632082. Fax: +48126340515. E-mail:broniato@chemia.uj.edu.pl.

interface.[25] In this technique, the composition of the monolayer and the ordering of the film-forming molecules can be strictly controlled by a researcher.[26,27] On the contrary, such manipulations are not possible in the above-mentioned investigations of surfactant vesicles. For at least 90 years, the interactions of different metal cations on different surfactants organized in Langmuir monolayers have been studied.[28] Heavy metals, such as cadmium and lead, can augment the ordering of film-forming molecules by the interactions with polar headgroups of the surfactants.[29,30] Especially, cadmium salts are used to increase the stabilization of Langmuir monolayers, mainly formed by carboxylic acids, while transferred on solid substrates with the Langmuir–Blodgett method.[31] Looking at a large pile of publications concerning the interactions of different ions with Langmuir monolayers, a surprising fact can be noticed: the interactions of the mercury salts dissolved in the water subphase with surfactant molecules in a Langmuir monolayer have not been researched whatsoever, to the best of our knowledge.

The idea of our present investigations is as follows: we have selected four film-forming molecules, having the same alkyl chain length (18 carbon atoms) and differing in the kind of a polar headgroup; namely, stearic acid, octadecylamine, octadecanethiol, and octadecanol have been chosen, as they possess in their molecules the physiologically important polar headgroups. The interactions between these surfactants spread in a Langmuir monolayer with mercury(II) nitrate have been studied in the first step of our investigations. Since one can suspect that the Hg^{2+}–surfactant interactions may be affected by anions present in the aqueous solution, therefore, different mercury salts (chloride, nitrate, acetate, bromide, and perchlorate) have been selected and applied in our study. To verify if the observed surfactant–mercury interactions are specific only to this very metal or similar to other heavy metals, some experiments have been repeated substituting the mercury(II) salts solutions by lead(II) nitrate, silver nitrate, and cadmium nitrate. The polar headgroups selected for our studies (carboxylic, amine, sulfhydryl, and hydroxyl) are the most important functional groups, which can be found in proteins as well as in membrane lipids. The aim of this selection was to verify if the sulfhydryl group is the only mercury-binding site or if there are other important functional groups that can be targeted by Hg^{2+} cation.

In our studies we have applied Langmuir technique, i.e., the surface pressure–mean molecular area (π–A) isotherm registration together with the measurements of electric surface potential. In addition, the structure of monolayers was visualized during the experiments with Brewster angle microscopy (BAM).

Experimental Section

Chemicals. The salts mercury(II) chloride (>99.5%), mercury(II) nitrate monohydrate (98.5%), mercury(II) acetate (99%), mercury(II) bromide (98%), lead(II) nitrate (99%), silver nitrate (99.5%), and cadmium chloride dihydrate (99%) were purchased from Fluka, whereas mercury(II) perchlorate hydrate (99.998%) and cadmium nitrate tetrahydrate (99.99%) were supplied by Aldrich. The surfactants stearic acid (99.5%), octadecylamine (99%), and octadecanol (99.5%) were purchased from Fluka, while octadecane-1-thiol (98%) was supplied by Aldrich. As the above-mentioned chemicals were of the highest commercially available purity, and they were applied as delivered, without any further purification. Chloroform (99.9%) HPLC grade was purchased from Aldrich and used as received. Ultrapure Milli-Q water of the resistivity higher than 18.2 MΩ·cm was used for the preparation of the solutions of the

investigated salts as well as the subphase in the Langmuir experiments.

Surface Pressure and Electric Surface Potential Measurements. The experiments were carried out on the symmetrical barrier NIMA 611 trough and on the NIMA 601 BAM trough (for BAM experiments) (NIMA, Coventry, UK). Solutions of the investigated surfactants of the concentrations of ca. 0.5 mg/mL were prepared in chloroform. In a typical experiment, an appropriate amount of the chloroform solution of the studied surfactant (ca. 10^{17} surfactant molecules) was spread on the surface of the salt solution or pure water (depending on the kind of experiment) with the Hammilton microsyringe. Ten minutes were allowed for the evaporation of chloroform, after which the monolayer was compressed with the compression velocity of 0.02 nm^2/(molecule min) (20 cm^2/min). In a set of preliminary measurements it was verified that the compression speed ranging within 10–40 cm^2/min does not affect the experimental results. The surface pressure was monitored continuously by a Wilhelmy electronic microbalance with an accuracy of 0.1 mN/m, using filter paper made of Whatman ashless chromatographic paper as the pressure sensor. The Langmuir trough was thermostated with a Julabo circulating water bath with an accuracy of 0.1 °C. All the experiments were carried out at 20 °C. A typical concentration of the mercury salts was 10^{-4} M; however, the effect of the concentration has been studied and it occurred that it is negligible within the range of 10^{-6} to 10^{-3} M.

Surface potential measurements were performed with the Kelvin probe (model KP2, NFT, Germany) mounted on a NIMA 611 trough. The vibrating plate was located ca. 2 mm above the water surface, while the reference electrode made of stainless steel plate was placed in the water subphase. The surface potential measurements were reproducible to ±10 mV. Both surface pressure–area and electric surface potential–area isotherms reported here are the averages of at least three experiments.

Brewster Angle Microscopy. Brewster angle microscope, BAM 2 plus (NFT, Germany), was used for microscopic observation of the monolayer structure. It is equipped with a 50 mW laser, emitting p-polarized light of 532 nm wavelength, which is reflected off the air–water interface at approximately 53.15° (Brewster angle). The lateral resolution of the microscope was 2 μm. The images were digitized and processed to obtain the best quality BAM pictures. Each image corresponds to a 770 μm × 570 μm monolayer fragment. All the applied equipment was placed on an antivibration table.

Results

We would like to start reporting our results from the description of the interactions of the four selected surfactants, namely, stearic acid, octadecylamine, octadecanol, and octadecanethiol, with mercury(II) nitrate. All the surfactants have the same length of the hydrocarbon aliphatic chain but differ in the character of the hydrophilic headgroup.

First of all, the π–A isotherms of the investigated surfactants were registered and the obtained curves are plotted in Figure 1. The π–A isotherms are in excellent agreement with the literature data as the studied here surfactants were already investigated before (π–A isotherms of stearic acid, ocdadecylamine and octadecanol measured at different experimental conditions can be found for example in the monograph by Gaines.[25] Data for octadecanethiol can be obtained in refs 32–34. In the second step, pure water subphase was exchanged for 10^{-4} M $Hg(NO_3)_2$ solution and the set of experiments was repeated. The resultant π–A isotherms are presented in Figure 1a–c as red lines. At

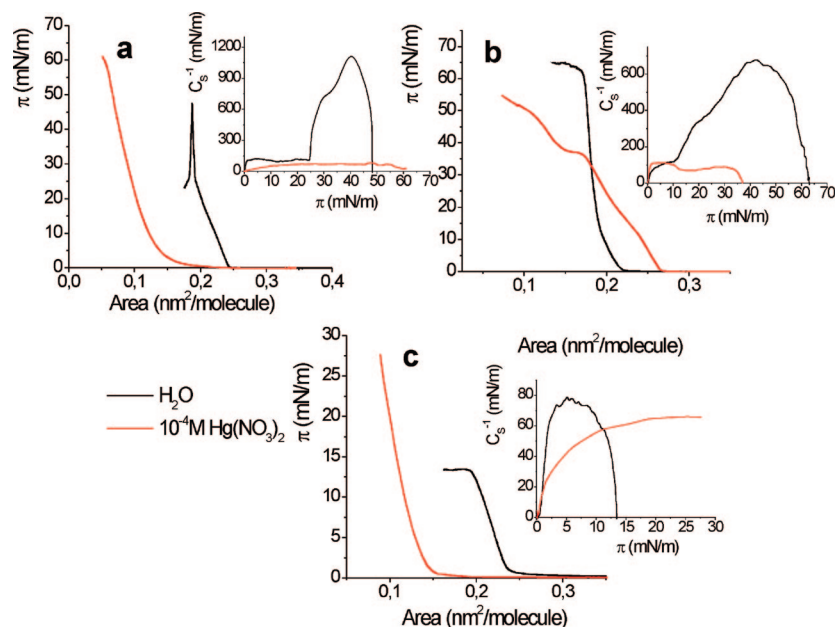Molecular Mechanism of Mercury Toxicity

J. Phys. Chem. B, Vol. 113, No. 13, 2009 **4277**

Figure 1. $\pi-A$ isotherms registered on pure water (black line) and on the 10^{-4} M Hg(NO$_3$)$_2$ solution (red line) for (a) stearic acid; (b) octadecylamine; and (c) octadecanethiol. Insets: $C_s^{-1}-\pi$ dependencies calculated from the respective $\pi-A$ isotherms.

first glance it can be noticed that the investigated molecules differ profoundly regarding their interactions with Hg(NO$_3$)$_2$. For stearic acid (Figure 1a) the isotherm registered on the 10^{-4} M Hg(NO$_3$)$_2$ solution has a completely different shape as compared with the reference isotherm obtained on pure water, and is shifted pronouncedly toward lower mean molecular areas, i.e., an initial increase of the surface pressure begins at ca. 0.15 nm^2/molecule vs 0.25 nm^2/molecule on pure water subphase. Upon further compression, the $\pi-A$ isotherm on Hg(NO$_3$)$_2$ solution increases smoothly without any changes in the slope, achieving high values of surface pressure and molecular areas lower than 0.1 nm^2 at its collapse. Knowing that the cross section of the aliphatic hydrocarbon chain is 0.185 nm^2,[25] it can be speculated that in the case of the spreading of stearic acid on 10^{-4} M solution of Hg(NO$_3$)$_2$, film-forming molecules do not form a monolayer but organize in a kind of a multilayer, in which the carboxylic groups bind the mercury(II) cations. Regarding octadecylamine monolayers (Figure 1 b), the $\pi-A$ isotherm registered on the 10^{-4} M Hg(NO$_3$)$_2$ solution is shifted toward larger mean molecular areas as compared to the isotherm on pure water. The isotherm is more expanded and has a plateau at ca. 35 mN/m, corresponding to a phase transition, after which at molecular areas below 0.15 nm^2/molecule further increase in the surface pressure can be noticed. The observed pronounced changes in the isotherm course indicate that there are important changes in the organization of the octadecylamine monolayer caused by the mercury(II) cations present in the subphase. However, as compared with stearic acid, the formation of a multilayer cannot be expected in this case; rather, a monolayer of a different organization is observed here. As far as octade-canol is concerned, the isotherms registered on water and on 10^{-4} M Hg(NO$_3$)$_2$ solution overlap, and a slight difference only in the collapse region can be noticed; therefore, these isotherms were not included in Figure 1. This observation can suggest that the interactions between the −OH group and Hg^{2+} cations are very weak, and due to this fact, the organization of molecules in the monolayer is very similar on both subphases. Finally, in Figure 1c the results gathered for octadecanethiol are presented. As the sulfhydryl group has a strong affinity toward the mercury(II) cations in aqueous solutions, significant changes

in the organization of the octadecanethiol monolayer on the Hg^{2+}-containing subphase can be expected. Therefore, the results presented in Figure 1c are not surprising. The isotherm registered on Hg(NO$_3$)$_2$ solution is shifted profoundly toward lower mean molecular areas and in some aspect is similar to the $\pi-A$ curve registered for stearic acid under the same experimental conditions. Thus, also for this compound it can be inferred that multilayer formation may occur in octadecanethiol film spread on the 10^{-4} M Hg(NO$_3$)$_2$ aqueous solution.

An important parameter derived from the $\pi-A$ isotherm, which can provide some additional information on the molecular organization in a monolayer, is the compression modulus C_s^{-1}, defined as $C_S^{-1} = -A\ d\pi/dA$. The value of C_s^{-1} higher than 250 mN/m indicates the solid state of a given monolayer, while lower values are typical for lower degree of order in the monomolecular film (namely $100-250$ mN/m is attributed to the liquid-condensed and $12-100$ to the liquid-expanded states of a Langmuir monolayer).[28] The C_s^{-1} values have been calculated for all the investigated isotherms discussed above, and the $C_s^{-1}-\pi$ plots are presented in the respective insets of Figure 1. From these dependencies it is clear that the cases of stearic acid and octadecylamine are very similar. For both compounds the monolayer has a solid character at least above the π value corresponding to the phase transition, whereas on the 10^{-4} M Hg(NO$_3$)$_2$ solutions the C_s^{-1} values are dramatically lower, indicating a lower degree of molecular organization. In the case of octadecanol, C_s^{-1} has slightly lower values on the mercury salt solution than on pure water; however, qualitatively, these differences are insignificant as in both cases the monolayer has a solid character above its phase transition, occurring at ca. 15 mN/m. The $C_s^{-1}-\pi$ dependence registered for octade-canethiol on water reveals the liquid-expanded character of its monolayer. The values of C_s^{-1} calculated for the monolayers of this chemical on Hg^{2+} solution do not differ qualitatively, indicating the same liquid-expanded state of the monolayer; however, in this case and for the monolayer of stearic acid in the presence of Hg^{2+} ions, the $C_s^{-1}-\pi$ dependence can be completely meaningless as the compression modulus is defined for monomolecular layers, while for both discussed here cases multilayer formation is very probable.
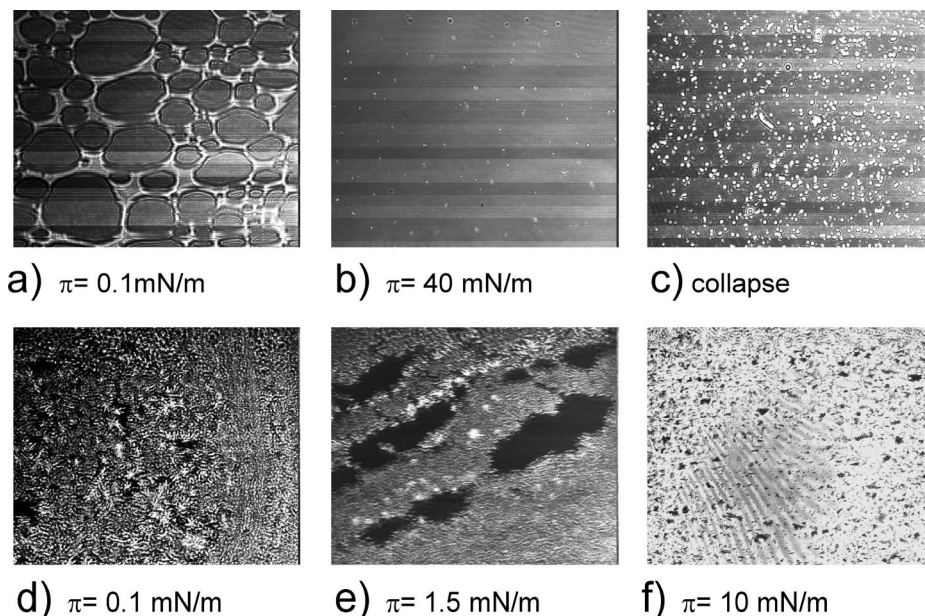
Figure 2. Representative BAM images observed for stearic acid monolayer on (a–c) pure water and (d–f) 10^{-4} M $Hg(NO_3)_2$.

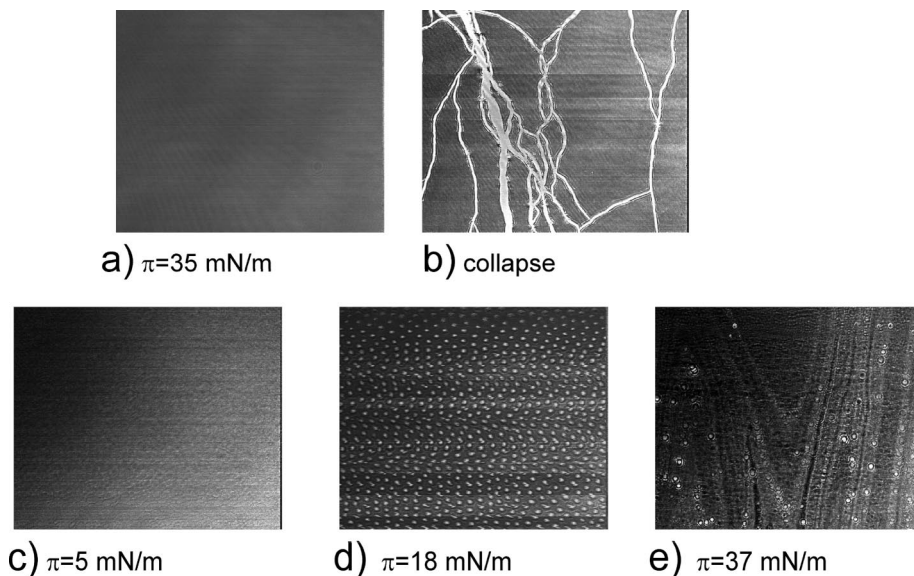**Figure 3.** Representative BAM images observed for octadecylamine monolayers on (a, b) pure water and (c–e) 10^{-4} M $Hg(NO_3)_2$.

The investigated monolayers were visualized with Brewster angle microscopy (BAM). The representative BAM images registered in these experiments are presented in Figures 2–4. Figure 2 shows BAM images taken for stearic acid on water (panels a–c) and on 10^{-4} M $Hg(NO_3)_2$ solution (panels d–f). The situation observed for the stearic acid monolayer on water was in accordance with different reports presented previously in the literature.[35,36] Generally, at the very beginning of the surface pressure rise, which corresponds to the gas–liquid expanded transition, the so-called foamlike structures can be observed (Figure 2a). Upon further compression, the monolayer is homogeneous within the limit of the BAM resolution, whereas at the monolayer collapse a multitude of bright spots, being 3D stearic acid crystals, can be observed. The situation changes dramatically on the $Hg(NO_3)_2$ solution/air interface. Even before the surface pressure rise, some gray islands differing in brightness can be observed, which can be ascribed to multilayer regions. Further compression causes the increase of the number of islands and their subsequent fusion; however, black areas also occur. Such a picture (Figure 2e) indicates that the

multilayer coverage is not homogeneous; and the observed black areas can be attributed to the region either not covered by the surfactant or having the monomolecular coverage. At surface pressures above 10 mN/m, the image becomes very bright, i.e., the thickness of the layer is increased, and no important changes can be noticed in BAM upon further pressure increase.

The representative BAM images registered for octadecylamine are presented in Figure 3. Panels a and b illustrate the monolayer structure spread on pure water, whereas three subsequent panels show the monolayer on $Hg(NO_3)_2$ solution. The monolayer of octadecylamine on pure water is homogeneous until the collapse, where bright long stripes of the collapsed material appear. On the contrary, on the $Hg(NO_3)_2$ solution at surface pressures higher than 10 mN/m, regularly ordered circular domains can be observed. At the collapse, diffused gray stripes encrusted with brighter circular domains are visible.

As far as octadecanol is concerned, BAM images are not shown since both on pure water and on $Hg(NO_3)_2$ surface the monolayers are homogeneous until the collapse, and even
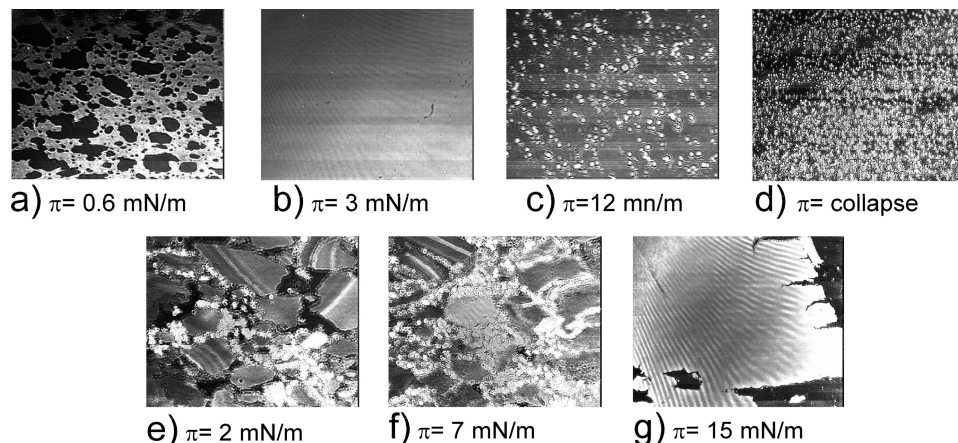
Figure 4. Representative BAM images observed for octadecanethiol monolayers on (a–d) pure water and (e–g) 10^{-4} M Hg(NO$_3$)$_2$.

beneath the collapse the structures are hardly noticeable and there are no visible differences between these two subphases.

Representative BAM images illustrating octadecanethiol films are shown in Figure 4. On pure water at surface pressures below 1 mN/m, structures typical for gas−liquid coexistence can be observed (Figure 4a), and upon further compression the monolayer remains homogeneous (Figure 4b); however, already below collapse at ca. 11 mN/m small bright points appear in the image (Figure 4c), indicating that the film collapse begins slightly before it is visible in the isotherm. Beneath the collapse, the image (Figure 4d) is similar to the previous one, with the difference that now 3D domains are more abundant. On the contrary, on Hg(NO$_3$)$_2$ solution/air interface, even at very low surface pressures, islands differing in shape, size, and brightness can be seen in the photo (Figure 4e). Upon compression, the number of these islands increases (Figure 4f), and their coalescence leads to the appearance of large areas of multilayer coverage (Figure 4g).

Another interesting and nontrivial problem, strictly connected with the interaction of the mercury(II) ions with the surfactant molecules organized in a Langmuir monolayer, is the influence of the anion. HgCl$_2$ and HgBr$_2$ have a distinct covalent character, which is manifested, for example, in their solubility; i.e., ca. 6 g of HgCl$_2$ can be dissolved in 100 g of H$_2$O, whereas more than 50 g can be dissolved in 100 g of acetone.[7] On the contrary, salts of mercury with oxoacid anions have more ionic character. For our investigations, the following salts have been selected: HgCl$_2$, Hg(NO$_3$)$_2$, Hg(CH$_3$COO)$_2$, HgBr$_2$, and Hg(ClO$_4$)$_2$. As it was proved previously, Hg^{2+} ions in the water subphase have virtually no effect on octadecanol monolayers, and therefore this compound was excluded from this part of investigations. The results obtained for different mercury(II) salts are gathered in Figure 5a−c.

Figure 5a presents the results for stearic acid. The $\pi-A$ isotherms are grouped into two categories: the isotherms measured on pure water and on the 10^{-4} M solutions of HgCl$_2$ and HgBr$_2$ are situated close to each other in the region typical for the monolayer coverage of the solution/air surface, whereas the $\pi-A$ isotherms registered on the solutions of Hg(NO$_3$)$_2$, Hg(CH$_3$COO)$_2$, and Hg(ClO$_4$)$_2$ virtually overlap and are situated at the low mean molecular areas typical for the multilayer coverage of the interface.

The situation observed for octadecylamine is considerably different and it seems that the amine molecules behave in an opposite way as compared with stearic acid. The isotherms registered on the 10^{-4} M Hg(NO$_3$)$_2$ and Hg(ClO$_4$)$_2$ exhibit more expanded character of the monolayer as the isotherms are shifted
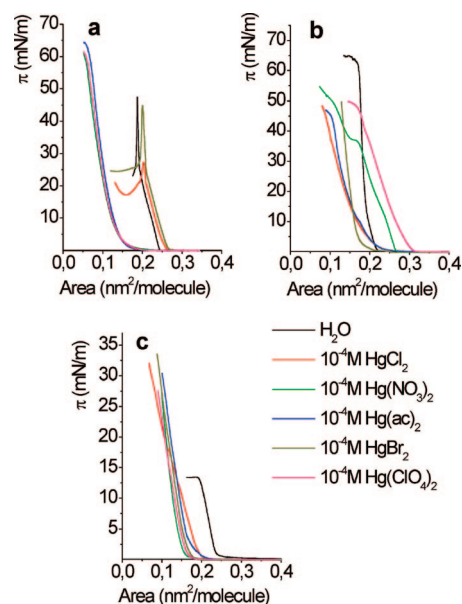

Figure 5. $\pi-A$ isotherms of the investigated surfactants: (a) stearic acid, (b) octadecylamine, and (c) octadecanethiol registered on different mercury salts.

to higher mean molecular areas and are less steep than the isotherm registered on pure water. Interestingly, the $\pi-A$ isotherms registered on the 10^{-4} M solutions of HgCl$_2$ and HgBr$_2$ are shifted toward much lower mean molecular areas and it can be inferred from their location that multilayer coverage of the interface is probable in these cases.

As far as the octadecanethiol monolayers are concerned, regardless of the type of the applied mercury salt, the isotherms are pronouncedly shifted toward mean molecular areas smaller than the cross section of the hydrocarbon chain, suggesting multilayer formation. It is another result differentiating the sulfhydryl group from the other functional groups investigated herein and indicating strong −SH−Hg^{2+} interactions, which cannot be affected by the presence of different counteranions in the water subphase.

To shed more light on the differences between the hydracid and oxoacid mercury(II) salts in their interactions with the investigated surfactants, changes of the electric surface potential have been monitored upon the compression and the resultant $\Delta V-A$ curves are gathered in Figure 6. We have focused our attention only on the monolayers of stearic acid and octadecylamine as for octadecanol and octadecanethiol the $\Delta V-A$ curves were practically identical, regardless of the applied mercury salt.
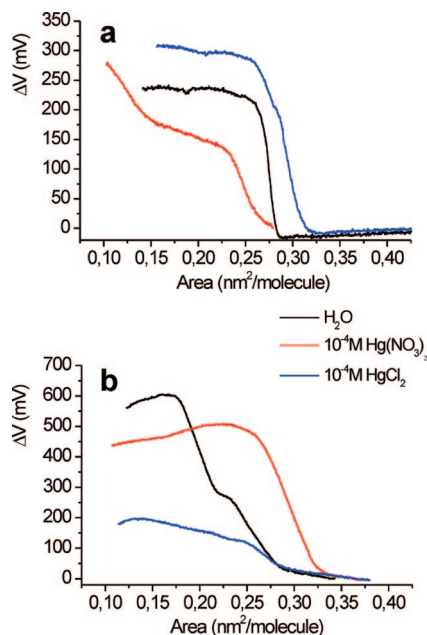
Figure 6. Surface potential ($\Delta V - A$) isotherms registered on different aqueous subphases for (a) stearic acid and (b) octadecylamine.

The surface potential starts to rise for both compounds at larger molecular areas than the $\pi - A$ isotherms and achieves a plateau approximately at molecular areas corresponding to the onset of the $\pi - A$ isotherms. Regarding the monolayers of stearic acid, the average value of the surface potential in this plateau is lower on the 10^{-4} M Hg(NO$_3$)$_2$ solution than on pure water and ca. twice as low as on the 10^{-4} M solution of HgCl$_2$. The trend observed for octadecylamine is reverse as the plateau region of the $\Delta V - A$ isotherm corresponds to twice as large surface potential value for the Hg(NO$_3$)$_2$ subphase than for HgCl$_2$. Generally, both the $\pi - A$ and $\Delta V - A$ isotherms indicate that the effect of the counterion of the mercury salt on the interaction of Hg^{2+} and $-$COOH or $-$NH$_2$ groups is of crucial importance, whereas for the $-$OH and $-$SH groups it is negligible.

As the $\Delta V - A$ isotherms suggested different organization of stearic acid and octadecylamine monolayers on HgCl$_2$-containing subphase than on the subphases containing oxoacid salts of mercury, the films were visualized with BAM (Figure 7).

It turned out that the texture of the stearic acid monolayer at the solution of HgCl$_2$ was practically the same as on pure water; whereas observations of the octadecylamine monolayer spread on the 10^{-4} M HgCl$_2$ solution revealed a situation which was considerably different from that observed in the measurements performed both on pure water and Hg(NO$_3$)$_2$ solutions. Even at a very small surface pressure value (Figure 7a), bright domains of different sizes are present. Upon the first steps of compression, the islands merge forming large regions of multilayer coverage, separated by the black background related to the uncovered surface. At higher surface pressure values, the whole field of view is bright; however, some black crevices in the multilayer can also be encountered as it happened in Figure 7c.

Finally, we thought that it would be interesting to spread the investigated surfactants on solutions of other heavy metals' salts as it could help to elucidate if the effects observed and described in this article are characteristic only of mercury(II) salts or perhaps they can be generalized for other heavy metal salts. As the representatives, Cd(NO$_3$)$_2$, Pb(NO$_3$)$_2$, and AgNO$_3$ were selected. The condensing effect of Cd^{2+} and Pb^{2+} on monolayers

from carboxylic acids is well documented in the literature,[29-31] and our results obtained here for stearic acid are in accordance with these reports (Figure 8a).

In contrast to Cd(NO$_3$)$_2$ and Pb(NO$_3$)$_2$, silver nitrate behaves similarly to the oxoacid salts of mercury and shifts the $\pi - A$ isotherm toward low mean molecular areas, corresponding to the multilayer coverage of the surface. In the case of octade-cylamine (Figure 8b), the investigated three salts exert some effect on the shape of the $\pi - A$ isotherm; however, the monomolecular coverage is maintained until the collapse and there is no evidence of multilayer formation on any investigated subphase. Values of C_S^{-1} calculated from these isotherms reveal that the monolayers preserve their solid character at higher surface pressures values. As far as the thiol monolayers are concerned (Figure 8c), all the heavy metal salts applied herein have identical effect as the investigated mercury salts; i.e., they induce a multilayer formation.

Discussion

To the best of our knowledge, our contribution is the first attempt to apply the Langmuir monolayer technique in the studies of the interactions between mercury(II) cations and surfactants monolayers. Molecular membranes are dynamic bilayers built of phospholipids, cholesterol, and different membrane proteins; however, a Langmuir monolayer can be treated as a half-membrane and applied as a practical model in studying of the interactions between molecular membrane and different chemicals.[26,27] For our investigations we have selected surfactants of different headgroups, $-$COOH, $-$NH$_2$, $-$OH, and $-$SH, which are of crucial importance in living cells, as they can be found in proteins, lipids, nucleic acids, and carbohydrates, i.e., in all the most important components of natural cells. The sulfhydryl group is frequently recognized in the literature as the main target of the Hg^{2+} ions, whereas other functional groups are often neglected in consideration of the mercury toxicity mechanism. Our results indicate that such an attitude to the problem of the molecular mechanism of mercury toxicity is an oversimplification. It turned out that from the investigated functional groups, only $-$OH does not form stable complexes with the investigated heavy metal cations, as the presence of different mercury(II) or other heavy metal salts in the water subphase does not affect the properties of octadecanol monolayers. We have also performed similar experiments for monolayers of cholesterol, as the sterol is also an alcohol, but similarly to octadecanol the presence of mercury(II) salts in the water subphase did not affect the physical properties of monolayers from cholesterol. On the contrary, the $-$COOH, $-$NH$_2$, and $-$SH head-groups interact strongly with mercury(II) salts.

The Hg^{2+} cation has a high affinity to the sulfur atom of the sulfhydryl group, which is a soft donor of a large polarizability. Most mononuclear mercury thiolate complexes have a low coordination number and exist as neutral linear dicoordinated complexes (Hg(SR)$_2$).[37-41] It can be inferred from our experimental data that such complexes are also formed by octade-canethiol and Hg^{2+} at the solution/air interface. The linear coordination of two octadecanethiol molecules by the Hg^{2+} cation leads to the formation of multilayer domains, which is proved by the observed shift of the isotherms toward low molecular area. As the coordination number of the [Hg(SH$-$C$_{18}$H$_{37}$)$_2$] complex is 2, no influence of the counterions from the mercury salt is observed, as they are not coordinated by the mercury atom.

There are many records of the Hg^{2+} carboxylate anion complexes in the literature. Very often a competition between
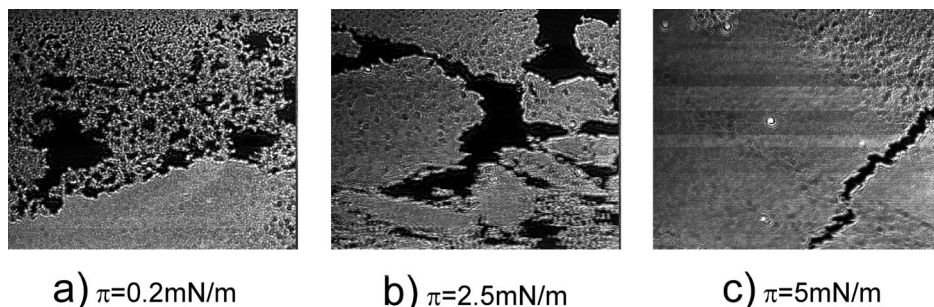
a) π=0.2mN/m   **b)** π=2.5mN/m   **c)** π=5mN/m

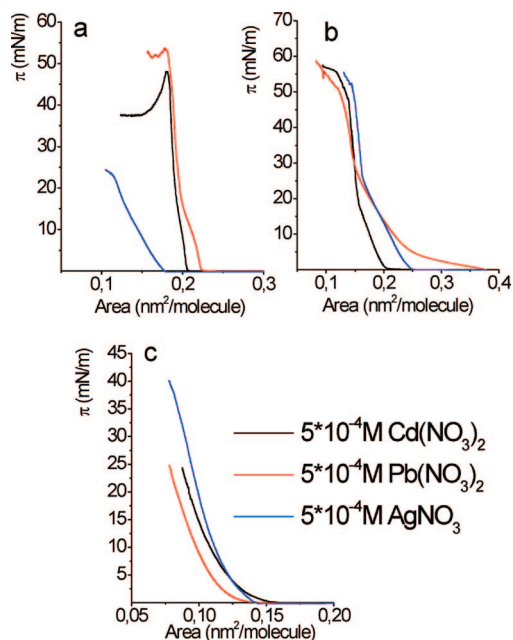**Figure 7.** BAM images observed for octadecylamine monolayers (a–c) on 10^{-4} M $HgCl_2$.

Figure 8. π–A isotherms registered for (a) stearic acid, (b) octadecylamine, and (c) octadecanethiol monolayers on 5×10^{-4} M $Cd(NO_3)_2$ (black curves), 5×10^{-4} M $Pb(NO_3)_2$ (red curves), and 5×10^{-4} M $AgNO_3$ (blue curves).

the –COO^- group and S or N donor atoms in multidentate ligands has been investigated.[42–44] Generally, mercury complexes with carboxylate ligands show a wide variety of coordination modes for the –COO^- group; however, the one where each carboxylate oxygen is singly coordinated to a different mercury atom is most common.[45] Our experimental results indicate that the Hg^{2+}–carboxylate complexes are also formed at the mercury salt solution/water interface. There is a profound influence of the anions present in the solution on the carboxylate coordination. The monolayers of stearic acid spread on $HgCl_2$ and $HgBr_2$ have their π–A isotherms similar to that registered on water, whereas the isotherms measured on $Hg(NO_3)_2$, $Hg(CH_3COO)_2$, and $Hg(ClO_4)_2$ are shifted profoundly toward lower mean molecular areas, similarly to the octadecanethiol monolayers spread on mercury salts, which indicates the multilayer formation. It is known from the literature that, when $HgCl_2$ or $HgBr_2$ reacts in aqueous solution with the carboxylate ligand, the halogen atoms are not eliminated and the complexes of the general formula $[HgX_2L]$ or $[HgX_2L_2]$ can be formed (where X is Cl or Br, and L is the carboxyl group).[43] The compression modulus (C_s^{-1}) calculated from the π–A isotherms of stearic acid spread on $HgCl_2$ and $HgBr_2$ solutions has lower values as compared with the monolayer spread on water; however, at higher surface pressure values all the monolayers have a solid character. Three is not a typical

coordination number of mercury;[46] therefore, it can be supposed that the real coordination number is 4 or 6, and that labile bonds with solvent molecules are formed, so the real formulas of these complexes formed at the solution/air interface can be $[HgX_2(H_2O)L]$ or $[HgX_2(H_2O)_3L]$. Different behavior of stearic acid on $Hg(NO_3)_2$, $Hg(ClO_4)_2$, and $Hg(CH_3COO)_2$ solutions originates from different coordination of mercury. The oxoacids' mercury salts have more ionic character and are ionized in aqueous solutions. Forming a carboxylate salt, mercury coordinates two carboxylic acid molecules $[HgL_2]$; however, one anion can also be coordinated and complexes of the type $[HgL_2(NO_3)]NO_3$ can be present at the solution/air interface.[47] Long-chain mercury carboxylates are very stable and the ionic exchange process of Hg^{2+} ion between two complex molecules is very slow. The linear coordination of two carboxylates to one Hg^{2+} cation facilitates multilayer formation and such disordered 3D islands are visible in BAM images of stearic acid spread on the $Hg(NO_3)_2$ solution. Regarding the electrical properties of the stearic acid monolayers spread on different Hg^{2+} salt solutions, the ΔV–A isotherms registered on pure water and on the 10^{-4} M solution of $HgCl_2$ are very similar, whereas the ΔV–A isotherm obtained on the 10^{-4} M $Hg(NO_3)_2$ differs profoundly as the plateau is reached at 150 mV, which is 100 mV lower than on pure water. The presence of ionic species in the $Hg(NO_3)_2$ solution makes the interpretation of the ΔV–A isotherm more difficult because the potential of the diffused double layer has also to be considered, as it is a part of the measured ΔV.

Let us now proceed to the interpretation of the amine headgroup–Hg^{2+} interactions. The complex formation between amine sp^3 nitrogen atom and mercury is well documented in the literature.[48–50] For example, amine-enriched polymeric resins were proposed as prospective tool in the purification of Hg^{2+}-contaminated off-waters.[51] It is visible in Figure 5b that the surface potential of the octadecylamine spread on pure water and on the $Hg(NO_3)_2$ solution achieves relatively high values of ca. 600 and 500 mV, respectively. These results suggest that in both cases the amine headgroup is protonated and bears the positive charge. It is not surprising, as it was mentioned in the literature that the pH measured in the bulk can be very different from the surface pH value, which is impossible to measure, but can be estimated with some models.[52] Repulsive interactions can be expected between the positively charged NH_3^+ headgroup and the solvated Hg^{2+} cation. Therefore, it seems that the Hg complexes, in which the NH_3^+–R molecule is a ligand, should have a rather labile character. This assumption together with the supposed repulsive interactions between the Hg^{2+} and octadecylamine monolayer leads to the conclusion that only one octadecylamine molecule can be coordinated in the system. All the above-mentioned trends lead to the observed lowering of the molecular ordering in octadecylamine monolayers when

spread on $Hg(NO_3)_2$ and $Hg(ClO_4)_2$, which is visible in the expansion of the $\pi-A$ isotherms shown in Figure 6b. In contrast to the mercury salts with oxoacids, the interactions between $HgCl_2$ and $HgBr_2$ with octadecylamine are very different. As has already been discussed above, the ionization of $HgCl_2$ and $HgBr_2$ in aqueous solutions can be ignored here, and in most cases Hg^{2+} does not lose halogen atoms while forming complexes with amines. As the $HgCl_2$ complex has no charge, there should not be repulsive interactions between its molecules and the ionized NH_3^+ groups at the solution/air interface. The pronounced lowering in the mean molecular area visible in Figure 5b suggests the formation of multilayer structures at the solution/air interface, and therefore it can be inferred that two amine molecules are coordinated, so the complexes have the formula $[HgX_2L_2]$. Moreover, the $\Delta V-A$ isotherm of octdecylamine measured on $HgCl_2$ is 3 times lower than the value recorded on water, as at the end of compression ΔV achieves the value of 200 mV only. It suggests that in the case of $HgCl_2$ coordination, the resulting monolayer of the complex is not charged, which also corroborates the proposed formula of the complex formed at the interface.

In comparison to the above-discussed results, the $\pi-A$ isotherms of stearic acid, octadecylamine, and octadecanethiol measured on cadmium, lead, and silver salts solutions are shown in Figure 8. The thiol forms similar complexes with all the investigated heavy metals as with mercury salts, which could have been predicted because thiols react readily with different transition metals, forming the $[M(SR)_2]$ complexes. Regarding the interactions with stearic acid, $AgNO_3$ behaves similarly to $Hg(NO_3)_2$, whereas the interaction of stearic acid molecules with Cd^{2+} and Pb^{2+} are distinctly different. The ions stabilize the monolayer of stearic acid below the transition pressure, causing that from ca. 10 mN/m on, the monolayer has a solid character, is better ordered, and is much more stable than the stearic acid monolayer at the water/air interface. This phenomenon can be explained by the formation of metal cation–surfactant crystalline superlatices at the solution/air interface.[31] In contrast to $HgCl_2$, $CdCl_2$ (and $Cd(NO_3)_2$) do not shift the octadecylamine isotherm to the regions typical for bilayers. It can be explained by the character of the cadmium halides, as they are much more ionic than mercury halogen salts and therefore are dissociated in their diluted aqueous solutions.

Conclusions

Long-chain carboxylic acids, amines, and thiols capable of Langmuir monolayer formation can form complexes with mercury salts dissolved in the aqueous subphase. Large differences between mercury halides and oxoacids salts have been noticed, which proves that the effect of the complex formation on monolayer properties depends on the character of the mercury salt. Octadecanethiol reacts at the solution/air interface with all the investigated mercury salts as well as with other heavy metals forming linear symmetrical complexes of coordination number 2. The presence of the mercury oxoacid salts in the aqueous solution causes the multilayer formation as the appearance of the stable mercury carboxylates is suggested, whereas in the presence of mercury halides the complexes of the general formula $[HgX_2L]$ can be formed, which lowers the degree of molecular ordering in the monolayer, but does not switch it to a multilayer film. The long chain amines tend to form stable, neutral complexes with mercury halides of the general formula $[HgX_2L_2]$ whereas, the complexes formed with the mercury oxoacid salts are labile and their formation leads to some destabilization of the octadecylamine monolayer. Our studies

indicated that apart from the SH–Hg binding, the Hg–COOH and Hg–NH₂ interactions could also be of great importance in the mechanism of mercury toxicity and its interaction with biological membranes, whereas the interactions of Hg^{2+} with cellular alcohols, such as for example cholesterol, seems to be negligible.

References and Notes

(1) Bickis, U. *Chem. Health Safety* **2001**, *8*, 19–24.
(2) Clarkson, T. W.; Magos, L.; Myers, G. J. *New England J. Med.* **2003**, *349*, 1731–1737.
(3) Grant, G. J. *Encyclopedia of Inorganic Chemistry*; J. Wiley & Sons: New York, 1994; pp 2136–2145.
(4) Breitinger, D. K. *Comprehensive Coordination Chemistry II*; Elsevier: Amsterdam, 2004; Vol. 6, pp 1253–1286.
(5) Gad, S. C. *Encyclopedia of Toxicology*; Elsevier: Oxford, UK, 2005; Vol. 3, pp 36–39.
(6) Son, M. H.; Kang, K. W.; Lee, C. H.; Kim, S. G. *Toxicol. Lett.* **2001**, *121*, 45–55.
(7) Rooney, J. P. K. *Toxicology* **2007**, *234*, 145–156.
(8) Gopal, K. V. *Neurotoxicol. Teratol.* **2003**, *25*, 69–76.
(9) Monnet-Tschudi, F.; Zurich, M. G.; Honegger, P. *Brain Res.* **1996**, *741*, 52–59.
(10) Limke, T. L.; Atchison, W. D. *Toxicol. Appl. Pharmacol.* **2002**, *178*, 52–61.
(11) Büsselberg, D. *Toxicol. Lett.* **1995**, *82/83*, 255–261.
(12) Yeh, J. H.; Chung, H. M.; Hu, C. M.; Jan, C. R. *Life Sci.* **2004**, *74*, 2075–2083.
(13) Sabolić, I. *Nephron. Physiol.* **2006**, *104*, 101–114.
(14) Aleo, M. F.; Morandini, F.; Betton, F.; Tanganelli, S.; Vezolla, A.; Giuliani, R.; Steimberg, N.; Apostoli, P.; Mazzoleni, G. *Toxicol. Vitro* **2002**, *16*, 457–465.
(15) Zolla, L.; Lupidi, G.; Bellelli, A.; Amiconi, G. *Biochim. Biophys. Acta* **1997**, *1328*, 273–280.
(16) Pribush, A.; Meyerstein, D.; Meyerstein, N. *Biochim. Biophys. Acta* **2002**, *1558*, 119–132.
(17) Krane, C. M.; Melvin, J. E.; Nguyen, H. V.; Richardson, L.; Towne, J. E.; Doetschman, T.; Menon, A. G. *J. Biol. Chem.* **2001**, *276*, 23413–234120.
(18) Preston, G. M.; Jung, J. S.; Guggino, W. B.; Agre, P. *J. Biol. Chem.* **1993**, *268*, 17–20.
(19) Das, R. M.; Ahmed, M. K.; Oulton, M. R.; Mantsch, H. H.; Tsubai, T.; Scott, J. E. *Chem. Phys. Lipids* **1997**, *89*, 107–117.
(20) Garcia, J. J.; Martinez-Ballarin, E.; Millan-Plano, S.; Allue, C. H.; Fuentes, L.; Escanero, J. F. *J. Trace Elements Med. Biol.* **2005**, *19*, 19–22.
(21) Bridges, C. C.; Zalups, R. K. *Toxicol. Appl. Pharmacol.* **2005**, *204*, 274–308.
(22) Akermoun, M.; Testet, E.; Cassagne, C.; Bessoule, J. J. *Biochim. Biophys. Acta* **2002**, *1581*, 21–28.
(23) Girlault, L.; Boudou, A.; Dufoure, E. J. *Biochim. Biophys. Acta* **1997**, *1325*, 250–262.
(24) Suvalsky, M.; Ungerer, B.; Villena, F.; Cuevas, F.; Sotomayor, C. P. *J. Inorg. Biochem.* **2000**, *81*, 267–273.
(25) Gaines, G. L., Jr. *Insoluble monolayers at liquid-gas interfaces*; Interscience Publishers: New York, 1966.
(26) Brockman, H. *Curr. Opin. Struct. Biol.* **1999**, *9*, 438–443.
(27) Rosetti, C. M.; Maggio, B.; Oliveira, R. G. *Biochim. Biophys. Acta* **2008**, *1778*, 1665–1675.
(28) Harkins, W. D. *Physical Chemistry of Surface Films*; Reinhold: New York, 1952.
(29) Bala, T.; Prasad, B. L. V.; Sastry, M.; Kahaly, M. V.; Waghamare, U. V. *J. Phys. Chem. A* **2007**, *111*, 6183–6190.
(30) Boyanov, M. I.; Kmetko, J.; Shibata, T.; Datta, A.; Dutta, P.; Bunker, B. A. *J. Phys. Chem. B* **2003**, *107*, 9780–9788.
(31) Dupres, V.; Cantis, S.; Benhabib, F.; Perrot, F.; Fontaine, P.; Goldmann, M.; Daillant, J.; Konovalov, O. *Langmuir* **2003**, *19*, 10808–10815.
(32) Itaya, A.; Van der Auweraer, M.; De Schryver, F. C. *Langmuir* **1989**, *5*, 1123–1126.
(33) Bilewicz, R.; Majda, M. *Langmuir* **1991**, *7*, 2794–2802.
(34) Gupta, R. K.; Suresh, K. A.; Guo, R.; Kumar, S. *Anal. Chim. Acta* **2006**, *568*, 109–118.
(35) Teixeira, A. C. T.; Brogueira, P.; Fernandes, A. C.; Goncalves da Silva, A. M. P. S. *Chem. Phys. Lipids* **2008**, *153*, 98–108.
(36) Lee, Y. L.; Yang, Y. C.; Shen, Y. J. *J. Phys. Chem. B* **2005**, *109*, 4662–4667.
(37) Mah, V.; Jalilehvand, F. *J. Biol. Inorg. Chem.* **2008**, *13*, 541–553.
(38) Bramlett, J. M.; Im, H. J.; Yu, X. H.; Chen, T.; Cai, H.; Roecker, L. E.; Barnes, C. E.; Dai, S.; Xue, Z. L. *Inorg. Chim. Acta* **2004**, *357*, 243–249.

Molecular Mechanism of Mercury Toxicity

J. Phys. Chem. B, Vol. 113, No. 13, 2009 **4283**

(39) Cheesman, B. V.; Arnold, A. P.; Rabenstein, D. L. *J. Am. Chem. Soc.* **1988**, *110*, 6359–6364.

(40) Jalilehvand, F.; Leung, B. O.; Izadifard, M.; Damian, E. *Inorg. Chem.* **2006**, *45*, 63–73.

(41) Kato, M.; Kojima, K.; Okamura, T.; Yamamoto, H.; Yamamura, T.; Ueyama, N. *Inorg. Chem.* **2005**, *44*, 4037–4044.

(42) Popović, Z.; Matković-Čalogović, D.; Hasić, J.; Vikić-Topić, D. *Inorg. Chim. Acta* **1999**, *285*, 208–216.

(43) Popović, Z.; Matković-Čalogović, D.; Popović, J.; Vicković, I.; Vinković, M.; Vikić-Tpoić, D. *Polyhedron* **2007**, *26*, 1045–1052.

(44) Terkhi, M. C.; Taleb, F.; Gossart, P.; Semmoud, A.; Addou, A. *J. Photochem. Photobiol. A: Chem.* **2008**, *198*, 205–214.

(45) Gonzalez-Duarte, P.; Leira, A.; March, R.; Pons, J.; Clegg, W.; Solans, X.; Alvarez-Larena, A.; Piniella, J. F. *Polyhedron* **1998**, *17*, 1591–1600.

(46) Grondhal, L.; Hammershoi, A.; Sargeson, A. M.; Thöm, V. J. *Inorg. Chem.* **1997**, *36*, 5396–5403.

(47) Quiroz-Castro, E.; Bernes, S.; Barba-Behrens, N.; Tapia-Benavides, R.; Contreras, R.; Nöth, H. *Polyhedron* **2000**, *19*, 1479–1484.

(48) Leung, B. O.; Jalilehvand, F.; Mah, V. *Dalton Trans.* **2007**, 4666–4674.

(49) Niu, W.; Wong, E. H.; Weisman, G. R.; Hill, D. C.; Tranchemontagne, D. J.; Lam, K. C.; Sommer, R. D.; Zakharov, L. M.; Rheingold, A. L. *Dalton Trans.* **2004**, 3536–3547.

(50) Patra, G. M.; Goldberg, I. *Polyhedron* **2002**, *21*, 2195–2199.

(51) Atia, A. A.; Donia, A. M.; El-Enein, S. A.; Yousif, A. M. *Sep. Sci. Technol.* **2007**, *42*, 403–420.

(52) Dynarowicz-Łatka, P.; Cavalli, A.; Oliveira, O. N. *Thin Solid Films* **2000**, *360*, 261–267.

JP810339E